

Inhibition of c-Myc Oncoprotein Limits the Growth of Human Melanoma Cells by Inducing Cellular Crisis*

Received for publication, May 2, 2003, and in revised form, June 20, 2003
Published, JBC Papers in Press, June 24, 2003, DOI 10.1074/jbc.M304597200

Annamaria Biroccio^{‡§}, Sarah Amodei^{‡¶}, Anna Antonelli^{||}, Barbara Benassi[‡], and Gabriella Zupi[‡]

From the [‡]Experimental Chemotherapy Laboratory, “Centro di Ricerca Sperimentale,” Regina Elena Cancer Institute, 00158 Rome, Italy and the ^{||}Cellular Biotechnology and Hematology Department, University “La Sapienza,” 00185 Rome, Italy

Here, we show that inhibition of c-Myc causes a proliferative arrest of M14 melanoma cells through cellular crisis, evident by the increase in size, multiple nuclei, vacuolated cytoplasm, induction of senescence-associated β -galactosidase activity and massive apoptosis. The c-Myc-induced crisis is associated with decreased human telomerase reverse transcriptase expression, telomerase activity, progressive telomere shortening, glutathione (GSH), depletion and, increased production of reactive oxygen species. Treatment of control cells with L-buthionine sulfoximine decreases GSH to levels of c-Myc low expressing cells, but it does not modify the growth kinetic of the cells. Surprisingly, when GSH is increased in the c-Myc low expressing cells by treatment with N-acetyl-L-cysteine, cells escape crisis. To test the hypothesis that both oxidative stress and telomerase dysfunction are involved in the c-Myc-dependent crisis, we directly inhibited telomerase function and glutathione levels. Inactivation of telomerase, by expression of a catalytically inactive, dominant negative form of reverse transcriptase, reduces cellular lifespan by inducing telomere shortening. Treatment of cells with L-buthionine sulfoximine decreases GSH content and accelerates cell crisis. Analysis of telomere status demonstrated that oxidative stress affects c-Myc-induced crisis by increasing telomere dysfunction. Our results demonstrate that inhibition of c-Myc oncoprotein induces cellular crisis through cooperation between telomerase dysfunction and oxidative stress.

The proliferative potential of normal cells in culture is limited to a finite number of population doublings, a phenomenon known as cellular senescence or Hayflick limit (1) that is characterized by a large, flat morphology, telomere shortening, a high frequency of nuclear abnormality and induction of β -galactosidase activity (2, 3). Continued cell proliferation beyond the Hayflick limit and further telomere erosion culminates in a period of massive cell death termed crisis (3). The limited capacity of human cells to replicate is an important tumor-suppressive mechanism (4), indicating that cancer cells must overcome this obstacle and achieve proliferation immortality

* This work was supported by grants from Italian Association for Cancer Research, Ministero della Sanità, and CNR-MIUR. The costs of publication of this article were defrayed in part by the payment of page charges. This article must therefore be hereby marked “advertisement” in accordance with 18 U.S.C. Section 1734 solely to indicate this fact.

§ To whom correspondence should be addressed: Experimental Chemotherapy Laboratory, Regina Elena Cancer Institute, Via delle Messi d'Oro 156, 00158 Rome, Italy. Tel.: 39-06-52662569; Fax: 39-06-52662505; E-mail: biroccio@ifco.it.

¶ Recipient of a fellowship from Italian Foundation for Cancer Research.

before they can form malignant neoplasms. Direct experimental evidence implicates telomere erosion as a primary cause of cellular arrest (5, 6). Most cells with indefinite proliferative ability maintain telomeres through the expression of the catalytic subunit of the enzyme, the human telomerase reverse transcriptase (hTERT)¹ (7, 8), and the introduction of telomerase into normal human cells provides telomere maintenance, prevention of senescence or crisis, and extension of life span (5, 6). In the opposite type of experiment, inhibition of telomerase in established tumor cell lines induces telomere shortening, leading to chromosome end-to-end fusions, cell death, and eventually arrest of culture growth (9–11). Recent evidence suggests that although telomere length is an important trigger for the onset of senescence, increased telomere dysfunction results in a loss of chromosome end protection and induction of senescence state (12).

Telomere dysfunction is not an absolute requirement for the induction of senescence, because other kinds of damage can contribute to the process. Reactive oxygen species (ROS), products of normal cellular oxidative process (13), have been shown to be involved in senescence (14). Senescent cells are known to have higher levels of ROS than normal cells (15). Moreover, oxidative stress caused by sublethal doses of H₂O₂ (16) or hyperoxia (17) can force human fibroblasts to arrest in a senescent-like fashion (18–20). Overexpression of antioxidant genes such as superoxide dismutase or catalase and the maintenance of cell cultures in low oxygen environment extend lifespan (13, 21, 22). All of these results point to a strong correlation between telomere dysfunction and senescence, as well as between oxidative damage and senescence. Growth beyond the senescence checkpoint correlates with genetic lesions that interfere with one or more key cellular mortality pathways, most prominently Myc, Rb, and p53 (23, 24). This is consistent with the findings that either activation of oncogenes or loss of tumor suppressor function is necessary to override the repression of telomerase in primary somatic cells.

The c-myc oncogene has been implicated in the regulation of telomerase through its ability to induce the transcriptional activation of hTERT (25–27). By using melanoma-derived clones expressing low levels of c-Myc, we recently demonstrated that telomerase plays a critical role in the c-Myc-dependent tumorigenicity (28). We have also demonstrated that the down-regulation of c-Myc decreases the intracellular glutathione (GSH) content, resulting in apoptosis (29). In this

¹ The abbreviations used are: hTERT, human telomerase reverse transcriptase; ROS, reactive oxygen species; DN, dominant negative; NAC, N-acetyl-L-cysteine; BSO, L-buthionine sulfoximine; SA, senescence-associated; β -gal, β -galactosidase; TUNEL, terminal deoxynucleotide transferase-mediated dUTP nick end labeling; BrdU, bromodeoxyuridine; TRAP, telomeric repeat amplification protocol; TRF, terminal restriction fragment; GSH, glutathione; Dox, doxycycline.

paper we found that GSH depletion and telomere loss induced by c-Myc down-regulation cause the growth arrest of M14 human melanoma cells.

MATERIALS AND METHODS

Cell Culture—The stable transfectants expressing low levels of c-Myc protein (MAS51, MAS53, and MAS57) and the control clone (MN2) were previously obtained by transfecting M14 parental line with an expression vector carrying antisense *c-myc* cDNA and/or a neomycin selection marker gene (30).

The M14-derived doxycycline-inducible clones expressing either low c-Myc or the puromycin resistance gene were recently obtained by a double transfection with a commercial inducible TET-ON gene expression system (Clontech) consisting of two expression vectors, one a regulator and the other a response vector carrying *c-myc* cDNA in antisense orientation or only the selected marker (29). Doxycycline (Dox; 1 $\mu\text{g}/\text{ml}$) was administered every 24 h either in the clone carrying the empty vector (control clone) or in the c-Myc transfectant.

The M14-derived stable transfectants expressing low levels of telomerase activity (MDN2, MDN4, and MDN16) and the control clone (MV3) were previously obtained by transfecting the dominant negative form of hTERT (DN-hTERT) cDNA (kindly provided by Dr. Weinberg) or the puromycin resistance gene only (28).

Serial cell cultivation was done plating 10^5 cells on 6-cm-diameter dishes; 5 days later the total number of cells in the dish were counted, and 10^5 cells were replated again. This procedure was repeated for 18 *in vitro* passages. The increase in population doubling level (ΔPDL) was calculated according to the formula ($\Delta\text{PDL} = \log(n_f/n_0)/\log 2$, where n_0 is the initial number of cells, and n_f is the final number of cells).

5 mM *N*-acetyl-L-cysteine (NAC; Sigma) or 1 mM L-buthionine sulfoximine (BSO; Sigma), doses with no toxic effect on cell survival, were used. According to the different experiments, NAC or BSO was added to the culture 24 h after plating and left in the medium for 24 h. The cells were then washed and incubated with fresh medium for 4 days. This procedure was repeated every culture passage. Intracellular GSH content was measured by a colorimetric assay (Bioxytech GSH-400; Oxis International, Inc., Portland, OR), as described by the manufacturer.

Morphological Analysis—Senescence-associated β -galactosidase (SA- β -gal) staining was performed as described by Dimri *et al.* (2). Briefly, the cells were fixed with 2% glutaraldehyde in phosphate-buffered saline for 5 min at room temperature, washed in phosphate-buffered saline, and incubated for several hours in staining solution: 1 mg/ml 5-bromo-4-chloro-3-indolyl- β -D-galactoside (X-gal), 5 mM potassium ferrocyanide, 5 mM potassium ferricyanide, 2 mM MgCl_2 in phosphate-buffered saline, pH 6.0. The nuclei were stained with 1 $\mu\text{g}/\text{ml}$ Hoechst 22358, and cells were analyzed using a fluorescence microscope.

Detection of apoptosis was performed in cytospin preparation by terminal deoxynucleotide transferase-mediated dUTP nick end labeling (TUNEL) assay using the ApopDETEK *in situ* apoptosis detection kit (Enzo Diagnostic, New York, NY) as previously reported (28). The percentage of apoptotic cells was determined by microscopic examination of TUNEL-treated slide at $\times 200$. For each slide, five fields were examined, and 100 cells in each field were counted.

Flow Cytometric Analysis—Cell percentages in the different phases of cell cycle were measured by flow cytometric analysis of propidium iodide-stained nuclei as previously described (31) using CELLQuest software (Becton Dickinson, San Jose, CA).

The percentage of cells synthesizing DNA was measured by flow cytometry (Becton Dickinson) using bromodeoxyuridin (BrdU; Becton Dickinson) incorporation, as previously described (30). Briefly, the cells were labeled with BrdU at a final concentration of 10 μM for 24 h, and the analysis was carried out at the end of BrdU labeling. The cells were then incubated with 2 $\mu\text{g}/\text{ml}$ of mouse anti-BrdU (clone BMC 9318; Roche Applied Science) for 30 min at room temperature, and the BrdU-positive cells were revealed with fluorescein isothiocyanate-conjugated anti-mouse monoclonal antibody (1:20; Dako, SA, Glostrup, Denmark).

For ROS content, adherent cells were first assayed for viability and then incubated with 4 μM dihydroethidium (Molecular Probes, Eugene, OR) for 45 min at 37 $^\circ\text{C}$. After incubation, the cells were analyzed by flow cytometry.

Western Blot—Western blot and detection were performed as previously reported (30). Briefly, 40 μg of total proteins were loaded on denaturing SDS-PAGE. Immunodetection of c-Myc and hTERT proteins was performed by using mouse anti-c-myc monoclonal antibody (clone 9E10; Santa Cruz Biotechnology, Santa Cruz, CA; 1:1000 dilution) and rabbit anti-hTERT polyclonal antibody (clone L-20; Santa

Cruz Biotechnology; 1:100 dilution). To check the amount of proteins transferred to nitrocellulose membrane, β -actin was used as control. The relative amounts of the transferred proteins were quantified by scanning the autoradiographic films with a gel densitometer scanner (Bio-Rad) and normalized to the related β -actin amounts.

Telomeric Repeat Amplification Protocol (TRAP)—Telomerase enzyme activity was measured with the PCR-based TRAP kit (Intergen Company, Oxford, UK) according to the manufacturer's instructions. To define the sensitivity of the method and the semi-quantitative relationship between protein concentration and ladder band intensity, different amounts of protein extract (from 0.01 to 2 μg) were used for each cell line and for all assays. In all cases, the reaction products were amplified in the presence of a 36-bp internal TRAP assay standard, and each extract was tested for heat sensitivity. Each set of TRAP assay included a control reaction without extract.

Southern Blot—Total DNA was isolated using the standard procedure. For each sample, 15 μg of DNA were digested with 40 units of *Hinf*I and electrophoresed on 0.8% agarose gel. DNA was denatured, neutralized, transferred to a nylon membrane (Hybond N; Amersham Biosciences), and cross-linked with ultraviolet light. The membrane was hybridized with 5'-end [γ - ^{32}P]deoxyadenosine triphosphate-labeled telomeric oligonucleotide probe (TTAGGG) $_3$ at 42 $^\circ\text{C}$ for 2 h in a rapid hybridization buffer (QuikHyb hybridization solution; Stratagene, La Jolla, CA). After washing, the filters were autoradiographed (Hyperfilm-MP; Amersham Biosciences) with an intensifying screen at -80 $^\circ\text{C}$ for 24 h. The autoradiographs were scanned, and the mean telomere length was calculated as reported by Harley *et al.* (32).

Cytogenetic Analysis—To obtain chromosome preparation, the cells were incubated with 0.1 $\mu\text{g}/\text{ml}$ colcemid for 1 h and trypsinized, then incubated with hypotonic 0.075 M KCl for 20 min, fixed with methanol to acetic acid (3:1 v/v), dropped onto frosted microscope slides, and air-dried overnight. End-to-end fusions were evaluated in at least 50 Giemsa-stained metaphases from two simultaneously grown cultures for each line and each treatment. For all the experiments, metaphase preparations of the different cells were performed simultaneously under the same conditions. The χ^2 test was used for statistical analysis.

RESULTS

c-Myc Down-regulation Causes Growth Arrest of M14 Melanoma Cells—We previously generated stable M14 melanoma transfectants expressing low levels of c-Myc compared with control cells (30). By using these transfectants, we here observed that, starting from culture passage 7, their growth rate slowed down, and then they stopped proliferating. In contrast, the growth kinetic of control cells was unabated (Fig. 1A). This effect was accompanied by a reduction of BrdU incorporation (Fig. 1B); although control cells maintained a high and stable labeling with BrdU (approximately 100%), BrdU-positive cells decreased from approximately 90% to less than 10% in the c-Myc transfectants with the increasing of culture passages.

To demonstrate the specific role of c-Myc in this phenomenon, a M14-derived Dox-inducible c-Myc low expressing clone, recently generated (29), was used. As previously reported, after 72 h of Dox administration, the cells showed a reduction of c-Myc protein level by approximately 60% compared with uninduced cells. Decreased c-Myc protein expression following Dox administration caused a growth arrest during the *in vitro* passages (Fig. 2). On the contrary, control cells showed no change in growth. When Dox was removed in the Dox-induced cells, they exhibited a growth rate similar to that of uninduced cells or the control clone, from the eighth passage onwards. Consistent with this result, c-Myc expression (Fig. 2, *inset*) was lower in the Dox-induced cells than in the uninduced or control clone, and it increased following Dox withdrawal.

Dox-induced cells showed distinctive cell characteristics associated with crisis. As cells passaged, a progressively increased expression of SA- β -gal activity was observed in Dox-induced cells, whereas a negligible amount was found in uninduced cells (Fig. 3A). Moreover, although no alteration in phenotypic characteristics was observed in uninduced and Dox-induced cells at early passages, induced cells became enlarged, often contained multiple nuclei, and had a vacuolated cyto-

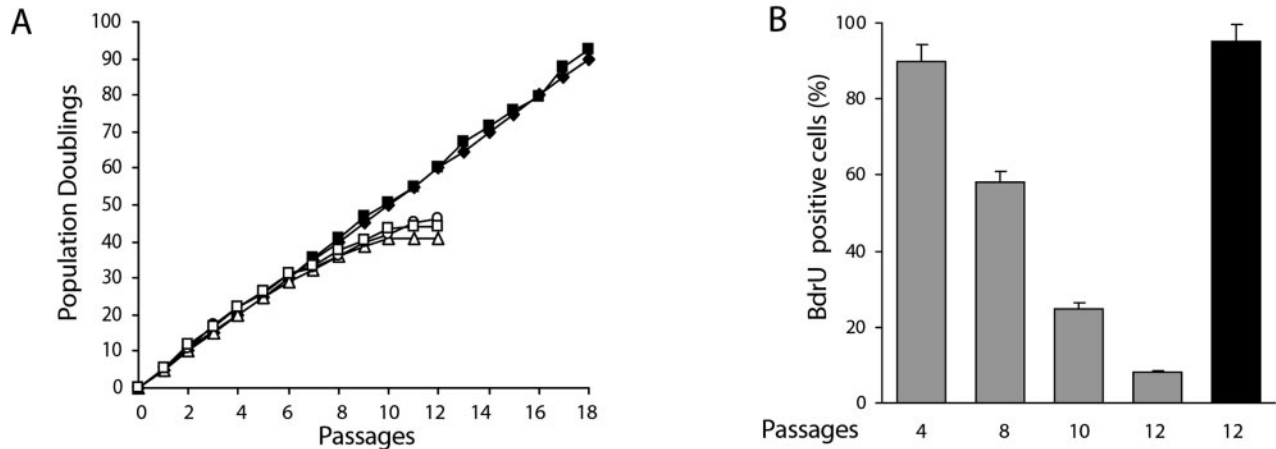


FIG. 1. **c-Myc down-regulation causes growth arrest.** A, growth of M14 parental line (■), MN2 control clone (◆), MAS51 (□), MAS53 (○), and MAS57 (△) c-Myc low expressing clones after serial culture passages. B, incorporation of BrdU in a representative c-Myc low expressing clone (gray bars) and in the control clone (black bar) at the indicated culture passages.

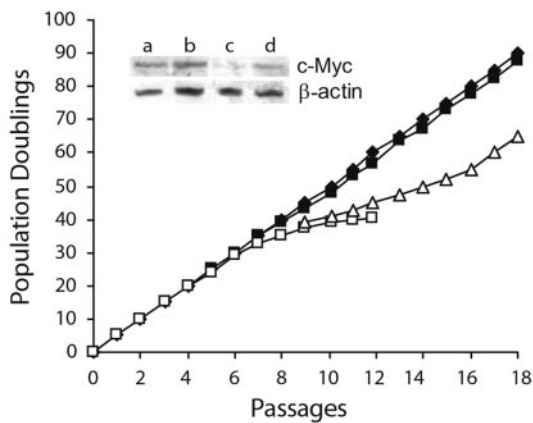


FIG. 2. **The growth arrest is a c-Myc-specific event.** Growth kinetics and Western blot analysis of c-Myc protein expression performed at passage 9 (inset) of M14-derived Doxycycline-inducible clones expressing either the control selected marker or low levels of c-Myc. Lane a and ◆, control clone; lane b and ■, uninduced c-Myc transfectant; lane c and □, Dox-induced c-Myc transfectant; lane d and △, Dox-induced c-Myc transfectant where Dox was removed since the eighth passage.

plasm from the eighth passage onwards (Fig. 3B, panel a). Cell cycle analysis revealed elevated forward and side scatters, which reflect increased cell size and granularity (Fig. 3B, panel b), and a cell cycle profile substantially altered (Fig. 3B, panel c). A significant decrease in the percentage of cells in G₁ phase was observed, which was the major factor contributing to a reduced ratio of G₁ to G₂/M cells. Staining of nuclei with Hoechst showed that cells contained multiple or multi-lobulated nuclei (Fig. 3B, panel d). These morphological characteristics predominated until day 5 of culture, and then apoptosis appeared (Fig. 3B, panel e). TUNEL staining detected an increase in the percentage of apoptotic cells with the increasing of culture passages, TUNEL-positive cells reaching 60% at the tenth *in vitro* passage.

c-Myc-induced Crisis Is Associated with an Impairment of Telomerase Function and Alteration of Intracellular Redox State—hTERT expression, telomerase activity, and telomere length were analyzed as functions of long term passage in culture. Western blot analysis (Fig. 4A), a semi-quantitative TRAP assay (Fig. 4B), and terminal restriction fragment (TRF; Fig. 4C) were performed in uninduced and Dox-induced c-Myc transfectant after four, eight, and ten *in vitro* passages. It is evident that hTERT protein expression and telomerase activity

were repressed in the Dox-induced cells compared with control cells. The decreased hTERT expression and telomerase activity were evident at the fourth passage, and they were unabated as cells passaged. Consistent with a reduction of telomerase activity, progressive telomere shortening occurred. As shown in Fig. 4C, TRFs length ranged from approximately 12 to 6 kb, with a mean length of approximately 8 kb in control cells. In contrast, in Dox-induced cells TRFs were significantly shorter already after 4 *in vitro* passages, ranging from 9 to 3 kb with a mean length of approximately 6 kb, and it reached a mean length of approximately 4 kb at the tenth passage.

c-Myc-induced crisis was also associated with alteration in the intracellular redox state. As reported in Fig. 4D, the value of GSH in Dox-induced cells was significantly lower ($p < 0.01$) than control cells. As a consequence, a significant increase in ROS production was observed (Fig. 4E). The measure of reactive oxygen species revealed that although no change in ROS content was evident in uninduced cells, approximately 30% of ROS was already found after four *in vitro* passages, and this percentage remained unchanged as cells passaged.

Restoration of Intracellular Glutathione Content Allows c-Myc Low Expressing Cells to Escape from Crisis—To determine whether the alteration of redox state influenced the c-Myc-dependent crisis, intracellular GSH content was normalized between control and c-Myc low expressing cells. In particular, control cells were treated with BSO, a specific inhibitor of GSH synthesis, to decrease the GSH levels, and in the opposite experiments, GSH levels were increased in the Dox-induced c-Myc cells by adding NAC, which is known to provide cysteine precursor for GSH synthesis. As shown in the Fig. 5A, the intracellular GSH content was significantly reduced in BSO-treated cells to levels comparable with c-Myc low expressing cells. Nevertheless, BSO-treated cells continued to proliferate, and the growth kinetic showed no change compared with untreated cells (Fig. 5B). NAC treatment of the c-Myc low expressing cells raised their GSH levels to those found in the controls (Fig. 5A), enabling the treated cells to continue proliferating, in contrast to the untreated cells (Fig. 5B). Moreover, NAC-treated cells escaped from crisis at late culture passages (Fig. 5C). In fact, the simultaneous analysis of SA-β-gal-positive and polinucleated cells revealed no significant difference between untreated and NAC-treated c-Myc transfectant at passage 8, the percentage of SA-β-gal-positive and polinucleated cells being approximately 40 and 10%, respectively, in all cells, regardless NAC treatment. On the contrary, as cells passaged, the difference between untreated and NAC-treated cells in

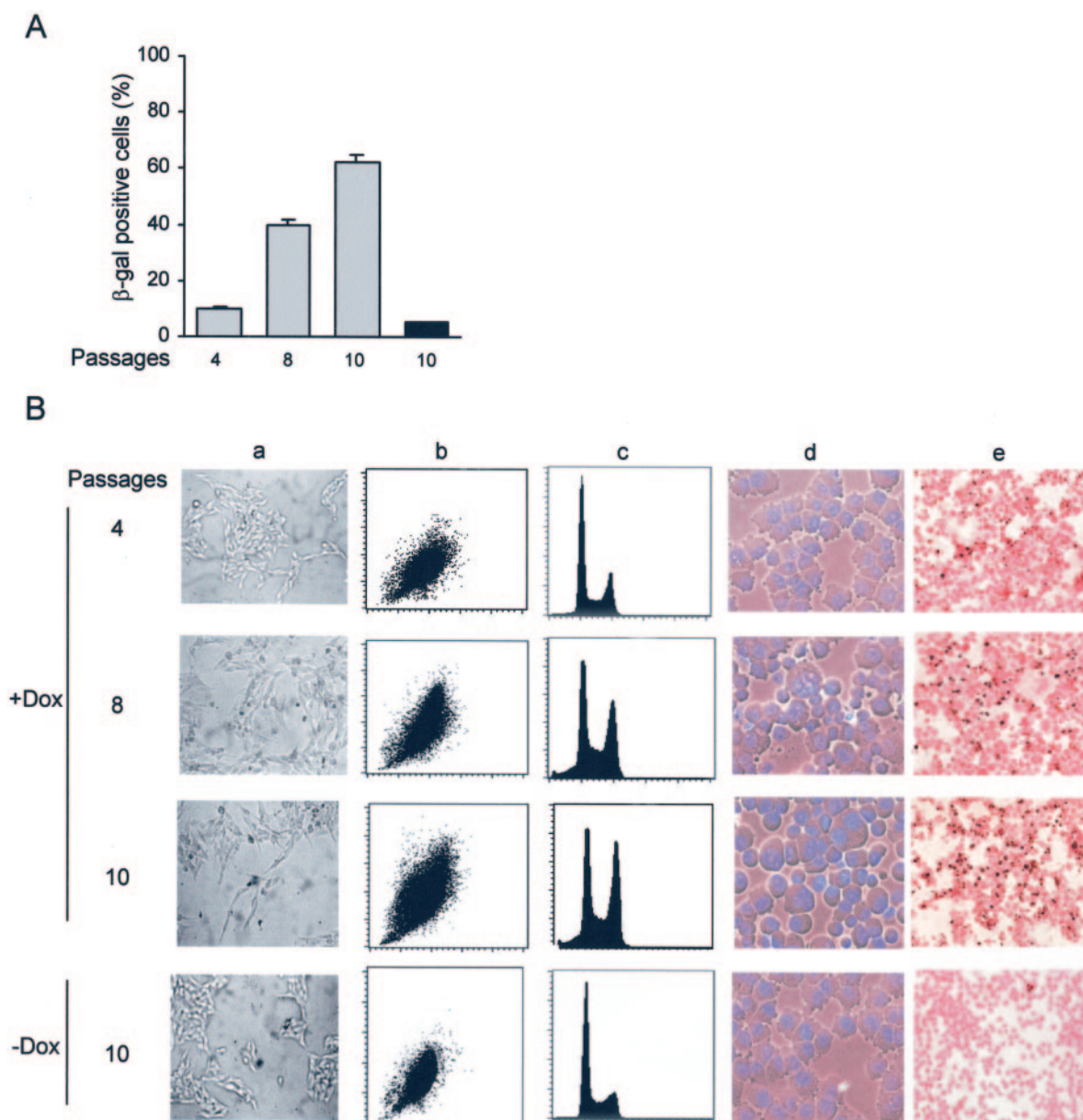


FIG. 3. **c-Myc down-regulation induces cellular crisis.** *A*, percentage of SA- β -galactosidase-positive cells in uninduced (black bar) and doxycycline-inducible c-Myc transfectant (gray bars) at the indicated culture passages. *B*, cellular morphology (panel *a*), cytofluorimetric dot plot of forward (*x* axis) and side (*y* axis) scatter parameters (*b*), DNA content analysis (panel *c*; *x* axis shows propidium iodide staining, and *y* axis shows cell number), Hoechst (panel *d*) and TUNEL (panel *e*) staining of uninduced ($-Dox$) and doxycycline-inducible c-Myc transfectant ($+Dox$) at the indicated culture passages.

terms of SA- β -gal-positive and polynucleated percentages became evident. In fact, whereas approximately 60% of SA- β -gal-positive cells were evident in the untreated cells at passage 10, a reduction by approximately 70% was revealed in the NAC-treated cells, and only a minimal presence of SA- β -gal activity existed at passage 18. Similarly, NAC treatment was able to significantly decrease the percentage of cells with supernumerary nuclei by approximately 75%, the percentage of polynucleated cells being approximately 25 and 5% in untreated and NAC-treated cells, respectively. In addition, the percentage of SA- β -gal-positive and polynucleated cells in NAC-treated cells at passage 18 was similar to that observed in control cells.

Glutathione Depletion Cooperates with Telomerase Dysfunction in Inducing Crisis—To test the hypothesis that oxidative stress could cooperate with telomerase dysfunction in the c-Myc-dependent crisis, we directly inhibited telomerase function and GSH levels. To this aim, an experimental model previously

generated (28), and consisting of three clones expressing a catalytically inactive DN-hTERT and a control clone expressing the puromycin gene only, was used. We first evaluated the effect of telomerase inhibition on growth properties (Fig. 6A). The growth kinetic of cells carrying a control retrovirus vector did not differ from those of parental cells (Fig. 1). In contrast, following DN-hTERT introduction, the cells displayed many characteristics of crisis, similar to what had been observed after c-Myc down-regulation (Figs. 1–3). In fact, as shown in Fig. 6B, the percentage of SA- β -gal cells in DN-hTERT cells progressively increased with the culture passages, reaching a value of approximately 70% at passage 14, whereas it remained lower than 5% in control cells.

As expected, DN-hTERT cells showed a reduction of telomerase activity by approximately seven times lower than control cells and telomere shortening (Fig. 6, C and D). On the contrary, no change in either c-Myc protein or intracellular GSH

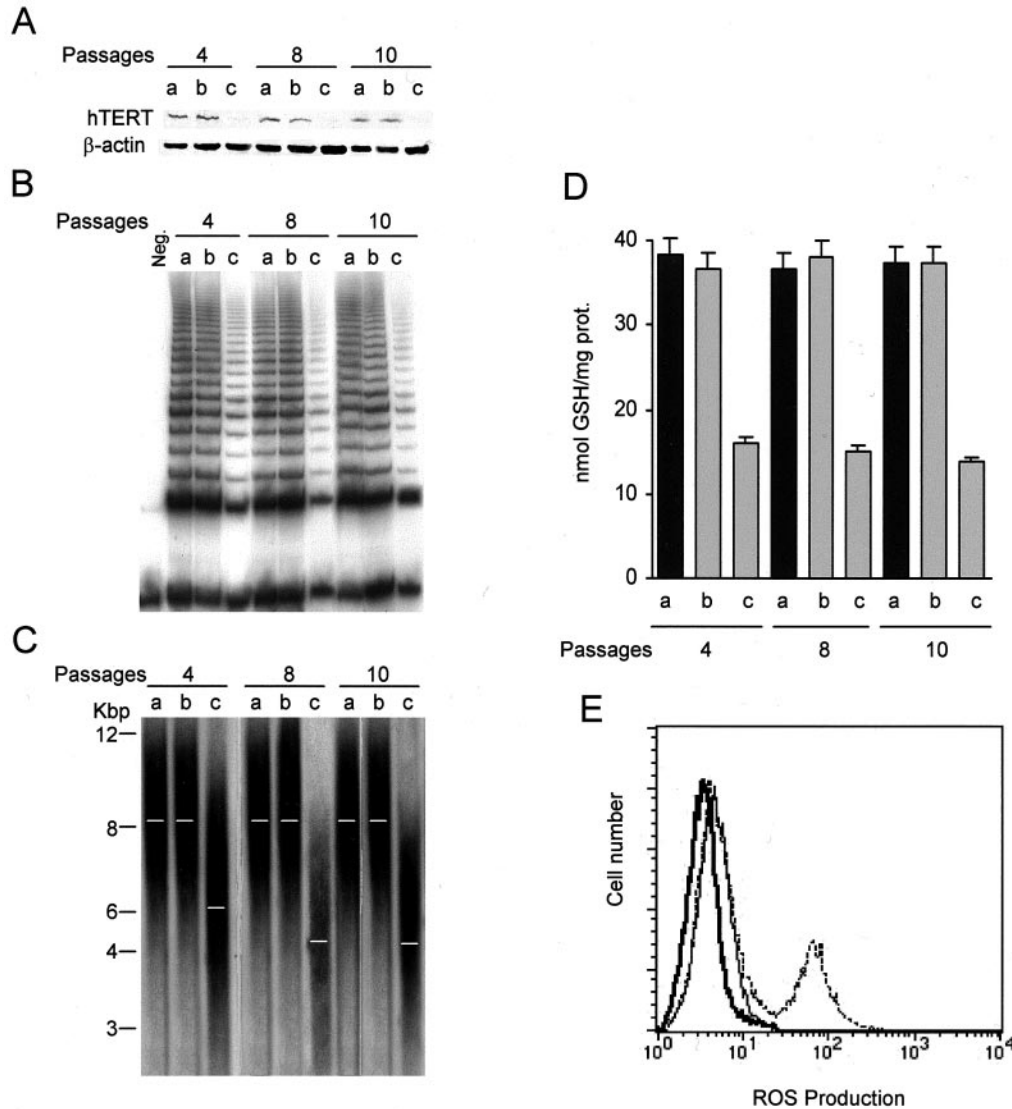


FIG. 4. *c-Myc*-induced crisis is associated with an impairment of telomerase function and oxidative stress. *A*, Western blot; *B*, TRAP assay; *C*, terminal restriction fragment; *D*, intracellular GSH content; *E*, flow cytometric analysis of ROS content in doxycycline-inducible clones expressing either the control selected marker or low levels of *c-Myc*. *Lanes a* and *bold line*, control clone; *lanes b* and *thin line*, uninduced *c-Myc* transfectant; *lanes c* and *dotted line*, Dox-induced *c-Myc* transfectant. *Kbp*, kilobase pair.

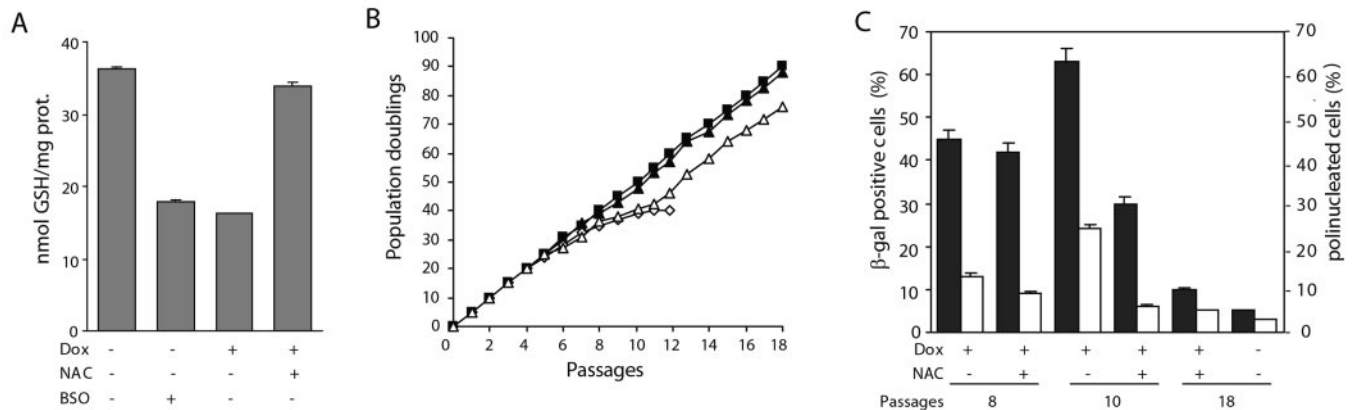


FIG. 5. Restoration of intracellular glutathione content reverts *c-Myc*-induced crisis. Intracellular GSH content (*A*) and growth kinetics (*B*) evaluated in uninduced *c-Myc* transfectant, left untreated (■) or treated with BSO (▲), and in Dox-induced *c-Myc* transfectant, untreated (◇) or treated with NAC (△). *C*, percentage of SA-β-galactosidase-positive (*black bars*) and polynucleated cells (*white bars*) at the indicated culture passages in uninduced and Dox-induced *c-Myc* transfectant, left untreated or treated with NAC.

content was observed between control and DN-hTERT cells (Fig. 6, *E* and *F*).

To demonstrate a cooperative effect between oxidative stress

and telomerase dysfunction, the intracellular GSH content was decreased in the DN-hTERT cells, and the growth kinetics of untreated and BSO-treated cells were monitored. BSO treat-

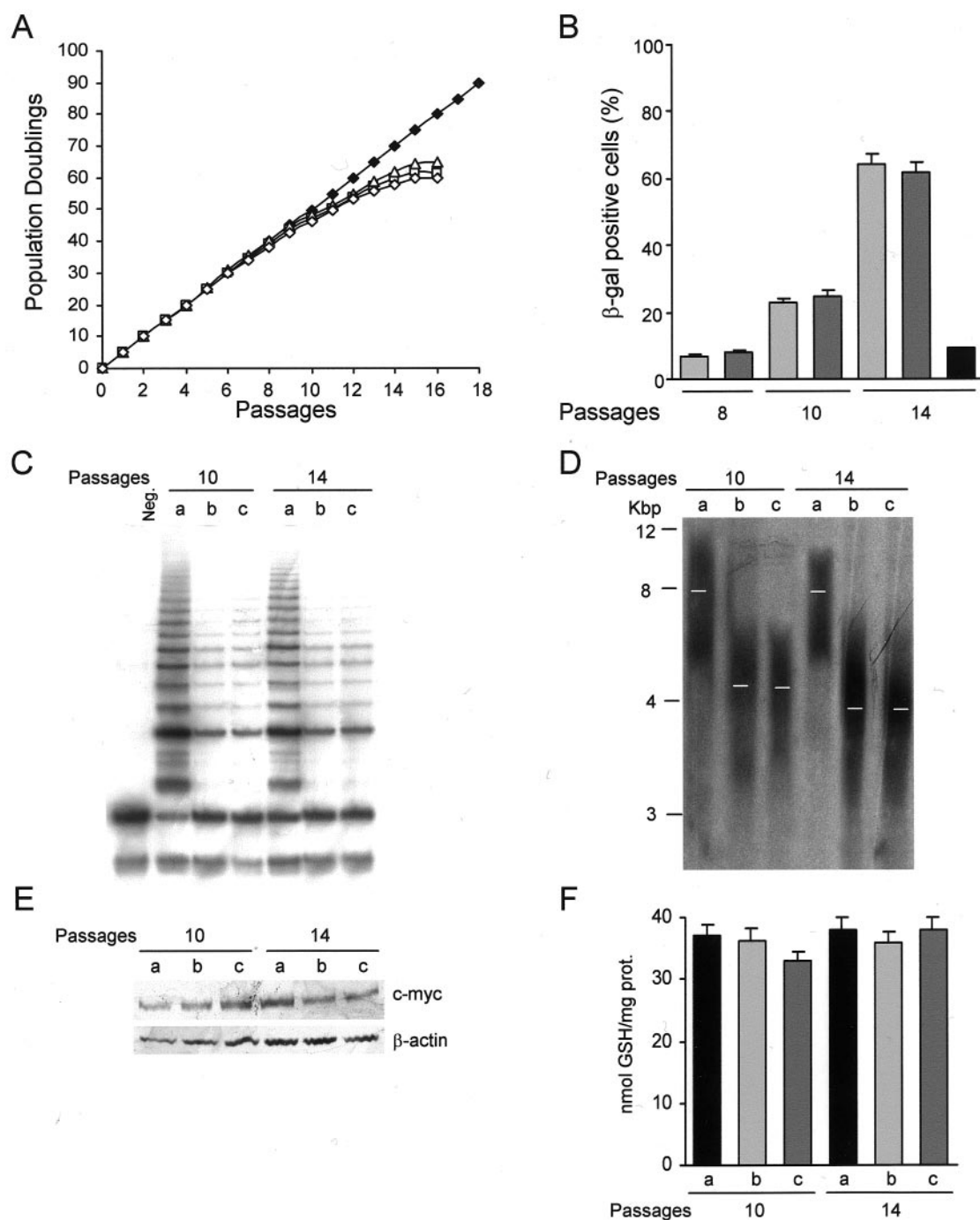


FIG. 6. **Inhibition of telomerase induces crisis.** *A*, growth of MV3 control clone (◆), MDN2 (□), MDN4 (◇), and MDN16 (△) DN-hTERT transfectants after serial culture passages. *B*, percentage of SA- β -galactosidase-positive cells in the control clone (black bar), MDN2 (light gray bars), and MDN4 (dark gray bars) DN-hTERT transfectants at the indicated culture passages. *C*, TRAP assay; *D*, TRF analysis; *E*, c-Myc protein expression; and *F*, intracellular GSH content in the control clone and in two DN-hTERT transfectants at the indicated culture passages. Lanes *a* and *b*, control clone; lanes *b* and *c*, MDN2 DN-hTERT transfectant; lanes *c* and *a*, MDN4 DN-hTERT transfectant. Neg., negative; Kbp, kilobase pair.

ment in DN-hTERT cells reduced the intracellular GSH content (Fig. 7A) to a level comparable with c-Myc transfectant (Fig. 5A) and accelerated the growth arrest induced by the inhibition of hTERT function (Fig. 7B). In fact, although DN-hTERT cells stopped proliferating after 16 culture passages, the BSO-treated cells had undergone growth arrest six passages before. These data were even more apparent from the analysis of SA- β -gal-positive and polynucleated cells evaluated at passage 10 (Fig. 7C). In fact, whereas approximately 70% of BSO-treated cells expressed β -gal, only 20% of β -gal-positive cells were present in the untreated DN-hTERT. Similarly, su-

pernumerary nuclei were increased in the BSO-treated cells, with untreated and BSO-treated cells having 10 and 25% nuclei, respectively.

Oxidative Stress Increases Telomere Dysfunction—To study how the change in the intracellular glutathione levels influences the c-Myc-dependent crisis, telomere status was analyzed. Fig. 8 shows terminal restriction fragment in the M14 parental line, in uninduced and Dox-induced c-Myc transfectant, both untreated and treated with NAC, and in DN-hTERT transfectants, both untreated and treated with BSO. In control and uninduced c-Myc transfectant, TRF length ranged from

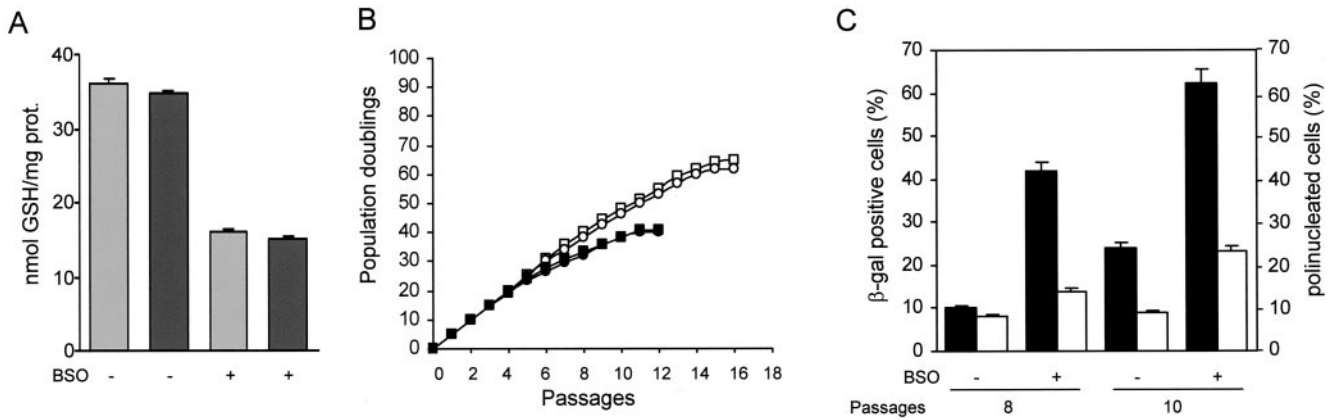


FIG. 7. **Oxidative stress cooperates with telomerase dysfunction in inducing crisis.** A, intracellular GSH content in MDN2 (light gray bars) and MDN4 (dark gray bars) DN-hTERT transfectants untreated or treated with BSO. B, growth of MDN2 and MDN4 DN-hTERT transfectants untreated (□ and ○) or treated with BSO (■ and ●). C, percentage of SA-β-galactosidase-positive (black bars) and polynucleated cells (white bars) in a representative DN-hTERT transfectant untreated or treated with BSO at the indicated culture passages.

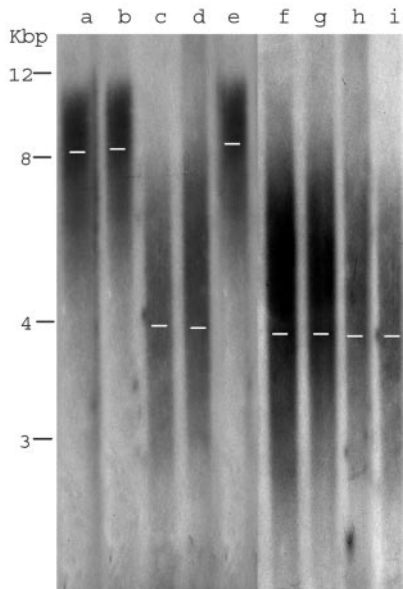


FIG. 8. **Oxidative stress does not alter telomere length.** Terminal restriction fragment in uninduced c-Myc transfectant untreated or treated with NAC (performed at passage 10) and in DN-hTERT transfectants untreated or treated with BSO (performed at passage 10). Lane a, control clone; lane b, uninduced c-Myc transfectant; lane c, Dox-induced c-Myc transfectant; lane d, Dox-induced c-Myc transfectant treated with NAC; lane e, MV3 control clone; lane f, MDN2 DN-hTERT transfectant; lane g, MDN2 DN-hTERT transfectant treated with BSO; lane h, MDN4 DN-hTERT transfectant; lane i, MDN4 DN-hTERT transfectant treated with BSO. Kbp, kilobase pair.

approximately 13 to 5 kb, with a mean length of approximately 8 kb. In contrast, TRFs in induced c-Myc transfectant were significantly shorter, ranging from 7 to 2 kb with a mean length of approximately 4 kb. Treatment of the c-Myc low expressing cells with NAC, capable of restoring intracellular GSH content and helping escape crisis (Fig. 5), did not modify telomere length. TRFs in c-Myc transfectant treated with NAC were superimposable to untreated cells. Similarly, in the opposite experiment, treatment of the DN-hTERT transfectants with BSO, capable of decreasing GSH levels and accelerating telomere-based crisis, did not alter the mean length of telomere. TRFs analysis, reported in Fig. 8, showed no significant difference in the mean of telomere length between DN-hTERT transfectants treated with BSO and those left untreated, the average being approximately 4 kb in both groups of cell, regardless of the GSH levels.

Data reported in Table I show that c-Myc transfectant had a high frequency of telomeric fusions when compared with control cells. A significant decrease in telomeric fusion frequency appeared in the c-Myc transfectant treated with NAC ($p < 0.0001$), when referred to untreated cells. The mean values of telomeric fusion frequency of untreated and NAC-treated c-Myc transfectant were 1.46 and 0.80, respectively. Similarly, DN-hTERT transfectants showed a higher frequency of telomeric fusions (approximately 1.4), compared with that in control clone (0.27). Treatment of the DN-hTERT transfectants with BSO significantly increased the number of telomeric fusions ($p < 0.0001$), BSO-treated cells harboring a total of 132 fusions of 61 metaphases analyzed.

DISCUSSION

Overexpression of the proto-oncogene c-myc has been associated with neoplastic transformation in a variety of malignant tumors (33). For human melanoma, c-Myc has been found to be an independent prognostic marker (34) correlated with clinical outcome in both primary and secondary disease (35–37). By blocking the expression of this gene, using an antisense approach, our group has largely documented the importance of the c-myc oncogene in controlling melanoma growth (38) and in sensitizing this tumor to chemotherapy (31, 39). In this paper we demonstrate that the down-regulation of c-Myc induces a proliferative arrest of melanoma cells after serial *in vitro* passages.

We first demonstrated that the growth arrest during the *in vitro* passages was a c-Myc-specific event by withdrawing doxycycline to increase c-Myc protein, which resulted in the return of cell proliferation. That c-Myc low expressing cells underwent crisis is indicated by their increase in size, the multiple nuclei, vacuolated cytoplasm, induction of senescence associated β-galactosidase activity, and massive apoptosis. The cellular crisis was associated with decreased telomerase activity through the ability of c-Myc to directly reduced hTERT protein expression and progressive telomere shortening. The observation that telomere progressively shortened with c-Myc down-regulation during the *in vitro* passages, which resulted in cell crisis, indicates that telomere shortening may play an active role in the crisis. This is further suggested by our previous findings that inducing telomere lengthening by restoring telomerase activity through exogenous expression of wild type and not the mutant biologically inactive hTERT is accompanied by reactivated cell proliferation and reversal of the reduced tumorigenic ability because of c-Myc down-regulation (28). Here, to test the hypothesis that telomerase dysfunction is involved in the c-Myc-

TABLE I
Oxidative stress increases telomere dysfunction

Lines	No. of cells analyzed	No. of cells with telomeric fusions						Total no. of telomeric fusions	Frequency of telomeric fusions ^a
		0	1	2	3	4	5		
c-Myc transfectants									
Control clone	61	45	15	1				18	0.29
Uninduced	56	42	13	1				17	0.30
Dox-induced	50	11	19	10	6	4		73	1.46
Dox-induced with NAC	65	26	28	9	2			52	0.80
DN-hTERT transfectants									
MV3	60	50	8	2				16	0.27
MDN2	56	11	20	19	6			76	1.36
MDN2 with BSO	61	8	9	18	19	6	1	132	2.16
MDN4	55	13	22	13	7			71	1.29
MDN4 with BSO	65	6	8	18	21	9	1	145	2.23

^a Calculated as total number of telomeric fusions/total number of metaphases analyzed.

dependent crisis, we directly inhibited telomerase function. We demonstrated that reducing hTERT catalytic function causes a phenotype similar to that observed after c-Myc down-regulation, with a reduced telomerase activity, shortened telomere, and cellular crisis. Our data are consistent with papers demonstrating that inhibition of telomerase in established tumor cell lines induces telomere shortening, cell death, and eventually culture growth arrest (9–11). It has been suggested that p53 is a participant in the cellular response to telomere disruption and loss (40, 41). In our experimental model, however, the c-Myc-dependent crisis does not appear to be dependent on functional p53. In fact, although the sequencing analysis of the p53 hot spots revealed that they were all wild type in M14 melanoma cells, the p53 oncoprotein was inactive because of its inability to transactivate the MDM2 or p21 promoters in a luciferase activity assay (data not shown). On the other hand, p53 mutations are rare in melanomas (42, 43), even if its pathway may be functionally inactivated (44).

Even though either inhibition of c-Myc or telomerase induces cellular crisis in M14 cells, the onset of cellular arrest was different between the c-Myc and DN-hTERT transfectants. By comparing the growth kinetics of c-Myc and DN-hTERT transfectants, a significant delay in the growth arrest was evident in the DN-hTERT. In fact, despite the levels of telomerase activity inhibition being absolutely comparable, c-Myc transfectants completely stopped proliferating after 12 culture passages, whereas DN-hTERT cells stopped after 16 passages. These data were corroborated by the analysis of β -galactosidase activity. These results suggested that, apart from the impairment of telomerase function, other mechanisms could contribute to the c-Myc-mediated crisis.

c-Myc down-regulation also induces an alteration in intracellular redox state, in terms of glutathione depletion and increased production of reactive oxygen species. The oxidative stress is not due to telomere erosion, because these two c-Myc-dependent biological effects are independent, c-Myc being able to affect two different target genes transcription: hTERT, the catalytic subunit of telomerase (25–27) and γ -glutamyl-cysteine synthetase, the enzyme for GSH biosynthesis (29). Here, we demonstrate that the alteration of these two different targets by c-Myc causes telomerase dysfunction and oxidative stress, both involved in the c-Myc-dependent crisis. The crucial role of redox state in the c-Myc-mediated crisis appears evident from the data obtained by modulating the GSH levels in the control and c-Myc low expressing cells. By treating control cells with BSO, an inhibitor of GSH synthesis, no modification occurred in the growth kinetic of cells. On the contrary, in the opposite experiment, GSH increase by NAC treatment in the c-Myc transfectant enabled cells to escape crisis. These results indicate that although oxidative stress is not sufficient to induce crisis, it is involved in the c-Myc-mediated cellular arrest.

Our data are in agreement with papers demonstrating that oxidative stress is involved in senescence (14) and that overexpression of antioxidant genes, such as superoxide dismutase or catalase, or the maintenance of cell cultures in low oxygen environment, causes extension of lifespan (13, 21, 22).

Moreover, the results demonstrating that modulation of GSH content has a significant effect on cellular crisis exclusively in the c-Myc low expressing cells, suggest that oxidative stress preferentially acts on dysfunctional telomeres. To test the hypothesis that both telomerase dysfunction and oxidative stress are involved in the c-Myc-mediated crisis, BSO treatment was used to decrease GSH content in the DN-hTERT transfectants. The GSH was reduced to levels comparable with those evaluated in c-Myc transfectants and the growth arrest induced by the inhibition of hTERT function accelerated, clearly demonstrating that both biological effects are involved in the c-Myc-dependent crisis. Analysis of telomere status, in terms of both telomere length and dysfunction, demonstrated that the change in the intracellular GSH levels influenced the c-Myc-dependent crisis by modulating telomere dysfunction rather than the mean telomere length. Our data are in agreement with recent evidence, suggesting that although telomere length is an important trigger for the onset of senescence, increased telomere dysfunction results in a loss of chromosome end protection and in an induction of senescence state (12). It has also recently been demonstrated that specific molecular alteration in telomere structure, such as the erosion of the telomeric single-strand overhang, occurs at senescence (45). All of these findings show that although length remains important, preservation of telomere integrity is critical, regardless of telomere length.

The results presented here have a therapeutic relevance. In fact, unlike most conventional chemotherapeutic drugs, agents that target telomerase may not induce cytotoxicity immediately after administration. This lag in therapeutic response will permit continued tumor cell growth for a period of time depending on the telomere length. Thus, the possibility of accelerating cell death by combining agents inducing telomerase dysfunction with drugs that cause oxidative stress may allow clinically important tumor response. The link between telomerase inhibition and oxidative stress may provide a basis for further studies employing a combination of inhibitors of telomerase and glutathione for cancer treatment.

Acknowledgments—We thank Adele Petricca for helpful assistance in typing the manuscript and Gael Ayers for language revision.

REFERENCES

- Hayflick, L. (1965) *Exp. Cell Res.* **37**, 614–636
- Dimiri, G. P., Lee, X., Basile, G., Acosta, M., Scott, G., Roskelley, C., Medrano, E. E., Linskens, M., Rubelj, I., Pereira-Smith, O., Peacocke, M., and Campisi, J. (1995) *Proc. Natl. Acad. Sci. U. S. A.* **92**, 9363–9367
- Wright, W. E., and Shay, J. W. (1992) *Exp. Gerontol.* **27**, 383–389

4. Vojta, P. J., and Barrett, J. C. (1995) *Biochim. Biophys. Acta* **1242**, 29–41
5. Bodnar, A. G., Ouellette, M., Frolkis, M., Holt, S. E., Chiu, C. P., Morin, G. B., Harley, C. B., Shay, J. W., Lichtsteiner, S., and Wright, W. E. (1998) *Science* **279**, 349–352
6. Vaziri, H., and Benchimol, S. (1998) *Curr. Biol.* **8**, 279–282
7. Counter, C. M., Avilion, A. A., LeFeuvre, C. E., Stewart, N. G., Greider, C. W., Harley, C. B., and Bacchetti, S. (1992) *EMBO J.* **11**, 1921–1929
8. Kim, N. W., Piatyszek, M. A., Prowse, K. R., Harley, C. B., West, M. D., Ho, P. L., Coviello, G. M., Wright, W. E., Weinrich, S. L., and Shay, J. W. (1994) *Science* **266**, 2011–2015
9. Hahn, W. C., Stewart, S. A., Brooks, M. W., York, S. G., Eaton, E., Kurachi, A., Beijersbergen, R. L., Knoll, J. H., Meyerson, M., and Weinberg, R. A. (1999) *Nat. Med.* **5**, 1164–1170
10. Zhang, X., Mar, V., Zhou, W., Harrington, L., and Robinson, M. O. (1999) *Genes Dev.* **13**, 2388–2399
11. Damm, K., Hemmann, U., Garin-Chesa, P., Huel, N., Kauffmann, I., Priepke, H., Niestroj, C., Daiber, C., Enenkel, B., Guilliard, B., Lauritsch, I., Muller, E., Pascolo, E., Sauter, G., Pantic, M., Martensm U, M., Wenz, C., Lingner, J., Kraut, N., Rettig, W. J., and Schnapp, A. (2001) *EMBO J.* **20**, 6958–6968
12. Karlseder, J., Smogorzewska, A., and de Lange, T. (2002) *Science* **295**, 2446–2449
13. Orr, W. C., and Sohal, R. S. (1994) *Science* **263**, 1128–1130
14. Chen, Q., Fischer, A., Reagan, J. D., Yan, L. J., and Ames, B. N. (1995) *Proc. Natl. Acad. Sci. U. S. A.* **92**, 4337–4341
15. Hagen, T. M., Yowe, D. L., Bartholomew, J. C., Wehr, C. M., Do, K. L., Park, J. Y., and Ames, B. N. (1997) *Proc. Natl. Acad. Sci. U. S. A.* **94**, 3064–3069
16. Chen, Q. M., Bartholomew, J. C., Campisi, J., Acosta, M., Reagan, J. D., and Ames, B. N. (1998) *Biochem. J.* **332**, 43–50
17. von Zglinicki, T., Saretzki, G., Docke, W., and Lotze, C. (1995) *Exp. Cell Res.* **220**, 186–193
18. Chen, Q., and Ames, B. N. (1994) *Proc. Natl. Acad. Sci. U. S. A.* **91**, 4130–4134
19. Calzini, R., Chevanne, M., Mocali, A., Tombaccini, D., and Paoletti, F. (1998) *Mech. Ageing Dev.* **105**, 137–150
20. Dumont, P., Burton, M., Chen, Q. M., Gonos, E. S., Frippiat, C., Mazarati, J. B., Eliaers, F., Remacle, J., and Toussaint, O. (2000) *Free Radical Biol. Med.* **28**, 361–373
21. Parkes, T. L., Elia, A. J., Dickinson, D., Hilliker, A. J., Phillips, J. P., and Boulianne, G. L. (1998) *Nat. Genet.* **19**, 171–174
22. Kinnula, V. L., and Hassinen, I. E. (1981) *Acta Physiol. Scand.* **112**, 387–393
23. Bishop, J. M., Eilers, M., Katzen, A. L., Kornberg, T., Ramsay, G., and Schirm, S. (1991) *Cold Spring Harbor Symp. Quant. Biol.* **56**, 99–107
24. Shay, J. W., Pereira-Smith, O. M., and Wright, W. E. (1991) *Exp. Cell Res.* **196**, 33–39
25. Wang, J., Ying Xie, L., Allan, S., Beach, D., and Hannon, G. J. (1998) *Genes Dev.* **12**, 1769–1774
26. Wu, K. J., Grandori, C., Amacker, M., Simon-Vermot, N., Polack, A., Lingner, J., and Dalla-Favera, R. (1999) *Nat. Genet.* **21**, 220–224
27. Greenberg, R. A., O'Hagan, R. C., Deng, H., Xiao, Q., Hann, S. R., Adams, R. R., Lichtsteiner, S., Chin, L., Morin, G. B., and DePinho, R. A. (1999) *Oncogene* **18**, 1219–1226
28. Biroccio, A., Amodei, S., Benassi, B., Scarsella, M., Cianciulli, A., Mottotese, M., Del Bufalo, D., Leonetti, C., and Zupi, G. (2002) *Oncogene* **21**, 3011–3019
29. Biroccio, A., Benassi, B., Filomeni, G., Amodei, S., Marchini, S., Chiorino, G., Rotilio, G., Zupi, G., and Ciriolo, M. R. (2002) *J. Biol. Chem.* **277**, 43763–43770
30. Biroccio, A., Benassi, B., Amodei, S., Gabellini, C., Del Bufalo, D., and Zupi, G. (2001) *Mol. Pharmacol.* **60**, 174–182
31. Citro, G., D'Agnano, I., Leonetti, C., Perini, R., Bucci, B., Zon, G., Calabretta, B., and Zupi, G. (1998) *Cancer Res.* **58**, 283–289
32. Harley, C. B., Fucher, A. B., and Greider, C. W. (1990) *Nature* **345**, 458–460
33. Nesbit, C. E., Tersak, J. M., and Prochownik, E. V. (1999) *Oncogene* **18**, 3004–3016
34. Grover, R., Pacifico, M. D., Wilson, G. D., and Sanders, R. (2003) *Ann. Plast. Surg.* **50**, 183–187
35. Kraehn, G. M., Utikal, J., Udart, M., Greulich, K. M., Bezold, G., Kaskel, P., Leiter, U., and Peter, R. U. (2001) *Br. J. Cancer* **84**, 72–79
36. Chana, J. S., Grover, R., Wilson, G. D., Hudson, D. A., Forders, M., Sanders, R., and Grobbelaar, A. O. (2001) *Ann. Plast. Surg.* **47**, 172–177
37. Chana, J. S., Grover, R., Tulley, P., Lohrer, H., Sanders, R., Grobbelaar, A. O., and Wilson, G. D. (2002) *Br. J. Plast. Surg.* **55**, 623–627
38. Leonetti, C., D'Agnano, I., Lozupone, F., Valentini, A., Geiger, T., Zon, G., Calabretta, B., Citro, G. C., and Zupi, G. (1996) *J. Natl. Cancer Inst.* **88**, 419–429
39. Leonetti, C., Biroccio, A., Candiloro, A., Citro, G., Fornari, C., Mottotese, M., Del Bufalo, D., and Zupi, G. (1999) *Clin. Cancer Res.* **5**, 2588–2595
40. Karlseder, J., Broccoli, D., Dai, Y., Hardy, S., and de Lange, T. (1999) *Science* **283**, 1321–1325
41. Chin, L., Artandi, S. E., Shen, Q., Tam, A., Lee, S. L., Gottlieb, G. J., Greider, C. W., and DePinho, R. A. (1999) *Cell* **97**, 527–538
42. Papp, T., Jafari, M., and Schiffmann, D. (1996) *J. Cancer Res. Clin. Oncol.* **122**, 541–548
43. Hartmann, A., Blaszyk, H., Cunningham, J. S., McGovern, R. M., Schroeder, J. S., Helander, S. D., Pittelkow, M. R., Sommer, S. S., and Kovach, J. S. (1996) *Int. J. Cancer* **67**, 313–317
44. Brantley, M. A., Jr., and Harbour, J. W. (2000) *Am. J. Pathol.* **157**, 1795–1801
45. Stewart, S. A., Ben-Porath, I., Carey, V. J., O'Connor, B. F., Hahn, W. C., and Weinberg, R. A. (2003) *Nat. Genet.* **33**, 492–496

Inhibition of c-Myc Oncoprotein Limits the Growth of Human Melanoma Cells by Inducing Cellular Crisis

Annamaria Biroccio, Sarah Amodei, Anna Antonelli, Barbara Benassi and Gabriella Zupi

J. Biol. Chem. 2003, 278:35693-35701.

doi: 10.1074/jbc.M304597200 originally published online June 24, 2003

Access the most updated version of this article at doi: [10.1074/jbc.M304597200](https://doi.org/10.1074/jbc.M304597200)

Alerts:

- [When this article is cited](#)
- [When a correction for this article is posted](#)

[Click here](#) to choose from all of JBC's e-mail alerts

This article cites 45 references, 18 of which can be accessed free at <http://www.jbc.org/content/278/37/35693.full.html#ref-list-1>